

# Enforced freedom: electric-field-induced declustering of ionic-liquid ions in the electrical double layer

Yufan Zhang,<sup>†</sup> Ting Ye,<sup>⊥</sup> Ming Chen,<sup>⊥</sup> Zachary A. H. Goodwin,<sup>§, ‡, ||</sup> Guang Feng,<sup>\*, ⊥</sup>  
Jun Huang<sup>\*, †</sup>, and Alexei A. Kornyshev<sup>\*, §, ||</sup>

<sup>†</sup> IEK-13, Institute of Energy and Climate Research, Forschungszentrum Jülich  
GmbH, 52425 Jülich, Germany

<sup>⊥</sup> State Key Laboratory of Coal Combustion, School of Energy and Power  
Engineering, Huazhong University of Science and Technology (HUST), Wuhan  
430074, China

<sup>§</sup> Department of Chemistry, Imperial College London, Molecular Sciences Research  
Hub, White City Campus, London W12 0BZ, U.K.

<sup>‡</sup> Department of Physics, Imperial College London, South Kensington Campus,  
London SW7 2AZ, U.K.

<sup>||</sup> Thomas Young Centre for Theory and Simulation of Materials, Imperial College  
London, South Kensington Campus, London SW7 2AZ, U.K.

<sup>+</sup> Hunan Provincial Key Laboratory of Chemical Power Sources, College of  
Chemistry and Chemical Engineering, Central South University, Changsha 410083,  
China.

\* E-mail: [gfeng@hust.edu.cn](mailto:gfeng@hust.edu.cn) (G.F.)

[jhuangelectrochem@qq.com](mailto:jhuangelectrochem@qq.com) (J.H.)

[a.kornyshev@imperial.ac.uk](mailto:a.kornyshev@imperial.ac.uk) (A.K.)

## **Abstract**

Ions in the bulk of solvent-free ionic liquids bind into ion pairs and clusters. The competition between the propensity of ions to stay in a bound state, and the reduction of the energy when unbinding in electric field, determines the portion of free ions in the electrical double layer (EDL). We present the simplest possible mean-field theory to study this effect. ‘Cracking’ of ion pairs into free ions in electric field is accompanied by the change of the dielectric response of the ionic liquid. The predictions from the theory are verified and further explored by molecular dynamics simulations. A particular finding of the theory is that the differential capacitance vs potential curve displays a bell shape, despite the low concentration of free charge carriers, because the dielectric response reduces the threshold concentration for the bell- to camel-shape transition. The presented theory does not take into account overscreening and oscillating charge distributions in the electrical double layer. But in spite of the simplicity of the model, its findings demonstrate a clear physical effect: a preference to be a charged monopole rather than a dipole (or higher order multipole) in strong electric field.

Keywords: ionic liquids, ion pairs, unbinding, differential capacitance

## Introduction

Electrochemical double layer (EDL) capacitors, also called supercapacitors, store energy by forming EDLs at electrodes.<sup>[1]</sup> They have significantly higher power density than conventional Li-ion batteries, because their charging process does not involve any electrochemical reactions, but just rearrangements of ions.<sup>[2]</sup> Owing to that they also have significantly longer operating life times, sustaining millions of charging-discharging cycles; whereas Li-ion batteries can only undergo only a few thousand cycles.<sup>[3]</sup> One of the priorities in supercapacitor research is the increase of energy density which is inferior to those of batteries. An avenue to rectify this is massively increasing the surface area of the electrode-electrolyte interfaces, by using micro- and mesoporous electrodes.<sup>[1]</sup> Another approach is the utilization of electrolytes that sustain higher applied voltages without undergoing electrochemical reactions. The exploit of ionic liquids (ILs), with their excellent thermal stability, nonvolatility, and relatively inert nature, enables one to attain higher operation voltages than aqueous and even organic electrolytic solutions, and thereby facilitates the storage of more energy.<sup>[4-6]</sup> Accurate theoretical description of the behavior of ILs in the EDL and, specifically of charge distribution and double layer capacitance, is a premise to understand their performance in supercapacitors (for review see Refs. 7 and 8).

Many modified Poisson-Boltzmann (PB) theories of the EDL, of different levels of complexity, have been put forward.<sup>[9-21]</sup> The majority of them model the system as ions embedded in a continuum medium with constant permittivity, which, as first pointed out by Debye, is insufficient to depict reality because the dielectric saturation effect on solvent polarizability is not considered.<sup>[22]</sup> Onsager, Kirkwood and Booth developed theories to account for this issue, that involved the

reduction of the dielectric constant of the solvent in the vicinity of electrode.<sup>[23-26]</sup> The dielectric constant affects how efficiently ions screen the electric field, and therefore it is closely related to the properties of the EDL, such as the differential capacitance ( $C$ ).<sup>[26-30]</sup> The reduced dielectric response of the solvent would generally result in a decreased  $C$ . Hence, more recently, researchers have modified their models to include the permanent dipoles and the excluded volume of solvents and ions, as well as the solvent quadrupolarizability.<sup>[31-36]</sup>

Little attention, however, has been put into the variation of the dielectric response in neat ILs with transient ion-pairing.<sup>[37, 38]</sup> In such a solvent-free system, the dielectric constant is predominantly contributed by transient ionic pairs and ions with dipole moments. Whereas Ref. 37 has studied the interchange between free and clustered ionic states, it is equally, if not more, important to study equilibria between such states in EDL, which is the subject of article.

In this work, we formulate a mean-field lattice-gas model of the EDL in a simplified IL system with consideration of the dipole moment of ion pairs, considering for simplicity the clustering at the ion pair level. This is, of course, a strong idealization, but it is a first step in this direction, which helps to elucidate the main qualitative effect: ‘liberation’ (declustering) of ions in the strong electric field of the double layer. This effect and the whole idea of the field-induced declustering is in spirit of the old classical Damaskin-Frumkin-Parsons cluster model of the compact layer capacitance in aqueous electrolytes.<sup>[39, 40]</sup> But we will explore its manifestations in the whole double layer of ionic liquid electrolytes.

Firstly, we derive an analytical expression for the field-dependent local dielectric constant ( $\epsilon_d$ ). Then, we describe the behavior of ion pairs in and out of EDL, followed by the comparison of the predicted number

density distribution of ions bound in ion pairs with the corresponding values obtained in molecular dynamics (MD) simulations. In addition, we investigate the behavior of differential capacitance as a function of electrode potential, which demonstrates a new trend in the “camel-bell transition”,<sup>[14]</sup> and is different from the prediction of the theory that does not take dielectric response into account.

The theory itself, should, of course, be taken with a ‘pinch of salt’: at best it can claim only qualitative results, as it does not incorporate the effect of overscreening and the decaying oscillations of charge density and electrical potential in the EDL.<sup>[7, 18]</sup> Therefore, the presented tests of its conclusions by MD simulations become critical.

## Methods

### *The model and mean-field theory*

We consider a system where ions exist in two states: free state and bound state, with interchange between them. For simplicity of analysis, we assume that cations and anions in free state are of the same size, monovalent with charge  $\pm e$  and do not possess permanent dipole moments (which, strictly speaking, can be true only for a limited number of ILs),<sup>[7]</sup> with their electronic polarizability determining an effective dielectric constant ( $\epsilon_e$ ) of a hypothetical ‘liquid of free ions’. Ions in the bound state, on the other hand, are assumed to be composed of cation-anion pairs; this ‘ion-pair’ assumption (i.e. avoiding special description of larger pairs) dramatically simplifies the formalism.<sup>[41]</sup> Because of the highly nonuniform charge density of ILs,<sup>[7, 42]</sup> the dipole moment of an ion pair is taken to be a fraction of the “full” dipole

moment, i.e.  $p = m \cdot e \cdot a$ , where  $a$  is the ion diameter (taken as 1 nm throughout this study), while  $m$  a coefficient between 0 and 1 (c.f. Ref. 40). We employ a lattice-gas model to depict such ‘ionic liquid’ in contact with a charged surface, as illustrated in Figure 1a.

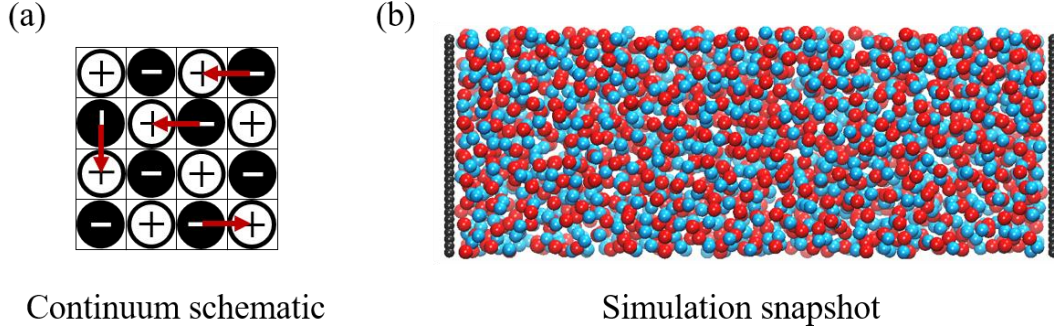


Figure 1. (a) Schematic of the lattice-gas description of the ionic liquids consisting of ‘free’ ions and those bound in ion pairs (red arrow). (b) Snapshot of the MD system with cations (red spheres) and anions (blue spheres). The cation and anion are defined as a bound-state ion pair when their ion centers are within a certain distance from each other, taking such distance to be the sum of the radii of the oppositely charged ions.<sup>[37]</sup>

The free energy functional for this lattice-gas model can be approximated as<sup>[14]</sup>

$$\begin{aligned}
F = \int d\mathbf{r} & \left( -\frac{1}{2} \epsilon_0 \epsilon_e E^2 + e\phi(n_+ - n_-) + f_{\text{free}}(n_+ - n_-) + f_{\text{bound}}(n - n_+ - n_-) \right. \\
& - \frac{1}{2} (n - n_+ - n_-) k_B T \ln \frac{\sinh\left(\frac{pE}{k_B T}\right)}{\frac{pE}{k_B T}} \\
& \left. - k_B T n_{\text{ref}} \ln \frac{\left(\frac{n}{n_{\text{ref}}}\right)!}{\left(\frac{n_+}{n_{\text{ref}}}\right)! \left(\frac{n_-}{n_{\text{ref}}}\right)! \left(\frac{n - n_+ - n_-}{2n_{\text{ref}}}\right)!} \right). \tag{1}
\end{aligned}$$

where  $\epsilon_0$  is the vacuum permittivity,  $\epsilon_e$  is the dielectric constant of IL constituted of free ions exclusively due to their electronic polarizability,  $E$  ( $E = -\nabla\phi$ ) is the electric field,  $\phi$  is the electrostatic potential,  $f_{\text{free}}$  and  $f_{\text{bound}}$  are the intrinsic free energy per free ion and bound ion,  $n_i$  is the number density of free ions ( $i = +, -$ ) in the unit of  $\text{nm}^{-3}$ ,  $n$  is the number density of total lattice sites, and  $n_{\text{ref}}$  is the reference number density ( $n_{\text{ref}} = 1/a^3$ ),  $k_B T$  is the thermal energy with  $k_B$  and  $T$  being the Boltzmann constant and absolute temperature, respectively.

The first term in Eq. (1) corresponds to the self energy of the electrostatic field while the second term denotes the electrostatic energy of free ions. Both terms are needed in order to derive the modified Poisson equation. From the third and fourth term, we can obtain the fraction of free ions in the bulk IL,  $\gamma$ , by the following equation analyzed in detail in Ref. 43,

$$f_{\text{free}} - f_{\text{bound}} + k_B T \ln \left( \frac{\gamma}{2(1-\gamma)} \right) = 0. \tag{2}$$

The fifth term accounts for the orientational contribution of ion pairs.

The last term in Eq. (1) describes the configurational entropy of the distribution of free ions and ion pairs on the lattice. We introduce  $n_{\text{ref}}$  to ensure a correct dimension. Its value will, of course, affect the magnitude of the free energy density,  $f$ , and electrochemical potential,  $\mu_i$ , but will not change the expression of the number density,  $n_i$ , and differential capacitance,  $C$ , as shown in the Appendix.

The number density of ions bound in ion pairs,  $n_{\text{bound}}$ , is derived by equalizing the electrochemical potential of each species ( $\mu_i = \partial f / \partial n_i$ ) with their counterparts in the bulk IL (analyzed in detail in the Appendix), and employing the relation  $n_{\text{bound}} = n - n_+ - n_-$ ,

$$\begin{aligned} \frac{n_{\text{bound}}}{n} &= \frac{(1 - \gamma) \left( \frac{\sinh(pE/k_B T)}{pE/k_B T} \right)^{\frac{1}{2}}}{\frac{\gamma}{2} \exp(-e\phi/k_B T) + \frac{\gamma}{2} \exp(e\phi/k_B T) + (1 - \gamma) \left( \frac{\sinh(pE/k_B T)}{pE/k_B T} \right)^{\frac{1}{2}}}. \end{aligned} \quad (3)$$

And the relation holds:  $\frac{n_{\text{bound}}}{n}|_{\text{bulk}} = 1 - \gamma$ . A detailed derivation of  $n_+$  and  $n_-$ , following the approach of Ref. 19, is shown in the Appendix.

The modified Poisson equation and the expression for field-dependent local dielectric constant are obtained by substituting the free energy functional into Euler-Lagrange equation  $\frac{\partial}{\partial x} \frac{\partial f}{\partial \phi'} - \frac{\partial f}{\partial \phi} = 0$ , analyzed in detail in the Appendix, and are given by,

$$\frac{d}{dx} \left( \epsilon_0 \epsilon_d \frac{d\phi}{dx} \right) = -e(n_+ - n_-), \quad (4)$$



$$\epsilon_d = \epsilon_e + \frac{(n - n_+ - n_-)p\mathcal{L}(pE/k_B T)}{2\epsilon_0 E}. \quad (5)$$

where  $\mathcal{L}(s) = (\coth(s) - 1/s)$  is the Langevin function.<sup>[32]</sup> The first term in Eq. (5) describes the electronic degrees of freedom of ions, and the second term originates from the orientational ordering of ion pairs. Through the factor  $(n - n_+ - n_-)$ ,  $\epsilon_d$  is affected by the interchange of ions between free and bound states.

### *Molecular dynamics simulations*

As shown in Figure 1b, our MD simulation system consists of two identical electrodes with a slab of IL enclosed between them. The distance between two electrodes is 30 nm, which is sufficiently large to ensure electroneutrality and bulk-like IL behavior in the middle of the system (not perturbed by the electrodes). The force fields of the electrodes and ILs are taken from Ref. 44; each electrode is made of Lennard-Jones (LJ) spheres arranged in a square lattice with a lattice spacing of 0.33 nm. The cations and anions of ILs are modeled as symmetrical LJ spheres with 1 nm diameter and opposite unit charge, i.e. the model of ions is also made as simple as possible to be able to compare it with the Coulomb lattice gas theory. The cation and anion are defined as a bound-state ion pair when their ion centers are within a certain distance from each other, and such distance was taken to be the sum of the radii of the oppositely charged ions.<sup>[37]</sup>

Simulations were performed in the NVT ensemble using the GROMACS package.<sup>[45]</sup> The temperature was maintained at 450K with Nosé-Hoover thermostat (the temperatures were elevated because ideal, identical size charged Lennard-Jones spheres tend to freeze at

room temperature). Particle-mesh Ewald (PME) summation, which is proposed by Darden to improve the performance of the reciprocal sum, was performed for computing long-range interactions (e.g., the electrostatic interactions).<sup>[46]</sup> In order to eliminate artifacts of the periodicity in the direction perpendicular to the electrodes, the length of the simulation box in this direction was set to be three times the width between the electrodes. The equilibration was performed for 5 ns with time step of 0.01 ps, following by another 20 ns production for further analysis.

The electrical potential distribution was calculated as,

$$\phi(z) = -\frac{\sigma}{\epsilon_0\epsilon_e}z - \frac{1}{\epsilon_0\epsilon_e} \int_0^z (z - z')\rho(z') dz'. \quad (6)$$

Here  $\sigma$  is the surface charge density,  $\epsilon_e$  is assigned value 2 in our simulations, and  $\rho$  is the ionic charge density along the direction perpendicular to the electrodes. Thus, the potential drop across the EDL ( $\phi_{\text{EDL}}$ ) is calculated relative to the potential of zero charge (PZC),<sup>[47]</sup>

$$\phi_{\text{EDL}} = (\phi_{\text{electrode}} - \phi_{\text{bulk}}) - (\phi_{\text{electrode}} - \phi_{\text{bulk}})|_{\text{PZC}}. \quad (7)$$

where  $\phi_{\text{electrode}}$  and  $\phi_{\text{bulk}}$  are, respectively, the potential on the electrode surface and in the bulk.

## Results and discussion

### *Number density profiles*

In what follows, we articulate the theoretical prediction in terms of the number density of ions bound in ion pairs,  $n_{\text{bound}}$ , and then compare it with our MD simulations. We set  $n_{\text{bound}}/n$  in bulk IL from theory the

same as that from simulations. In this case,  $n_{\text{bound}}/n$  in bulk IL are determined to be both 0.54, and the corresponding portion of free ions,  $\gamma$ , is 0.46, without invoking Eq. (2). The dipole moment of an ion pair is set as  $8.8 \times 10^{-29} \text{ C m}$  ( $0.45e \cdot a$ ) in order that  $\epsilon_d$  at bulk IL is around 15, the typical value.<sup>[7]</sup> Figure 2a,b show  $n_{\text{bound}}$  at different electrode potentials. The reader should not be worried that the shown range of electrode potentials is much wider than the typical electrochemical window for electrode potentials in ionic liquids, which is rarely larger than 3 V.<sup>[48, 49]</sup> The goal of going to such extremes, is to show the trend in de-clustering that would favor the monopole ions rather than ion pairs. Firstly, we focus on the  $n_{\text{bound}}$  profile at  $\phi_{\text{EDL}}$  being -8 V from the theory side, where it first increases and then decreases as approaching the electrode from the bulk. The hump in the  $n_{\text{bound}}$  profile is attributed to the presence of two competing forces affecting ion pairs: they tend to exist in regions of higher electric fields because of polarization, however, sufficiently high electric fields ultimately unbind the ion pairs into free ions.

In addition, Figure 2a shows that as a higher charge accumulates on the electrode, the unbinding of ion pairs causes the hump of  $n_{\text{bound}}$  profile to reside further away from the electrode, which, as depicted in Figure 2b, is corroborated by MD simulations. Particularly, the locations of the humps at -0.5 V (blue curve) and -5.5 V (orange curve) obtained from theory are in good agreement with those from MD simulations. It is worth reiterating that because of the local-density nature of our mean-field theory, the layered structure inherently revealed by the MD simulation cannot be captured, which explains why the single hump in theory continuously moves toward the bulk as the

electrode potential gets higher biased, whereas in simulations we see a layered structure of several humps, and their location is weakly affected by the electrode potential.<sup>[50]</sup>

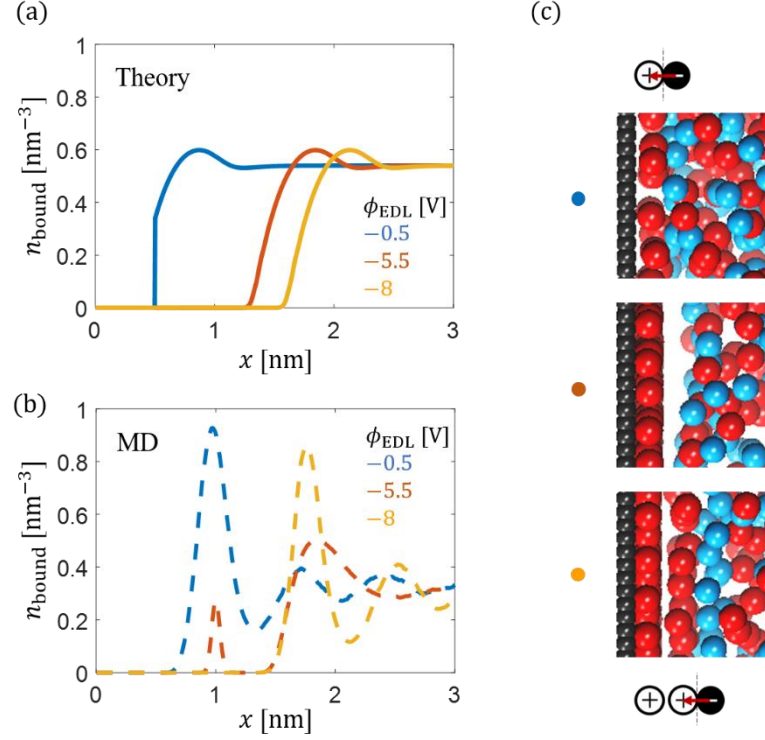


Figure 2. (a-b) The number density profiles of ion pairs obtained from theory (a) and MD (b), respectively.  $T = 450$  K,  $n_{\text{bound}}/n$  in bulk IL is 0.54 and the corresponding  $\gamma = 0.46$ . For the theory side,  $p = 0.55 \times ea = 8.8 \times 10^{-29}$  C m. For the MD side, the total number density of ions, both free and bound, in bulk IL is  $0.62 \text{ nm}^{-3}$  (lower than  $1 \text{ nm}^{-3}$  from the theory side). The fraction of ions bound in ion pairs in bulk IL is 0.54, and therefore the corresponding  $n_{\text{bound}}$  is  $0.34 \text{ nm}^{-3}$ . (c) Snapshots of the MD simulations performed at  $\phi_{\text{EDL}}$  being  $-0.5$  V (blue dot),  $-5.5$  V (orange dot) and  $-8$  V (yellow dot).

Figure 3 displays the theoretically obtained  $\epsilon_d$  [Eq. (5)] profile at  $-0.5$ ,  $-5.5$  and  $-8$  V. It is shown that  $\epsilon_d$  experiences a drastic decrease from 15 to almost 2 as approaching the electrode. This stems from the prediction that ion pairs unbind in the EDL, and therefore the dielectric

screening is reduced.

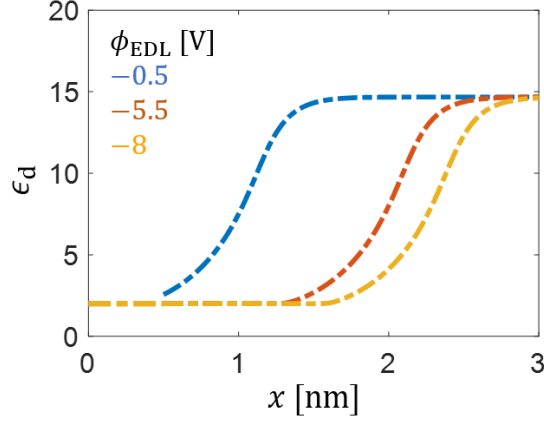


Figure 3. Field-dependent local dielectric constant profiles in the vicinity of the electrode with different potential drops obtained from theory. The parameters are set to be the same as those in Figure 2. The spatial variations of  $\epsilon_d$  originate from its dependence on field.

#### *Differential capacitance*

The traditional wisdom in the IL-based EDL theory articulates that the differential capacitance curve in the primitive model displays a camel shape if the fraction of free charge carriers in the bulk electrolyte is lower than  $1/3$ .<sup>[14]</sup> However, the incorporation of the ion pairs in the present model changes the threshold ( $\gamma = 1/3$ ) of the “camel-bell transition”. In this section, we investigate the differential capacitance vs potential ( $C - \phi_{\text{EDL}}$ ) curve of the case where  $\gamma$  is 0.2 (lower than  $1/3$ , different from 0.54 used in the previous section), and see if it displays a camel shape which is predicted by the primitive model. For the present and primitive models, we set  $\epsilon_d$  as 10.5 in bulk IL (different from 15 used in the previous section) and therefore the dipole moment of the present model is  $4.8 \times 10^{-29} \text{ C m}$  ( $0.3e \cdot a$ ). As revealed by Figure 4a, the present model may well show a bell-shaped  $C - \phi_{\text{EDL}}$  curve despite  $\gamma$  is lower than the  $1/3$  threshold, contrary to the camel-

shaped dashed curve predicted by the primitive model employed in Ref. 14. The model, of course, could give a  $C - \phi_{\text{EDL}}$  curve of camel shape, but the corresponding number density would be lower than  $1/3$  and dependent of the magnitude of  $p$ . On the other hand, the model gives a lower  $C$  than the primitive model,<sup>[14]</sup> which is explained by the reduction in the dielectric screening depicted in Figure 4b. No matter how the electrode is charged, the  $\epsilon_d$  at electrode-electrolyte interface,  $\epsilon_d^{\text{surf}}$ , remains unaltered in the primitive model. In the present model, however, ion pairs near the electrode-IL interface shift to free state, resulting a decreased  $\epsilon_d^{\text{surf}}$ .

This finding serves as a reminder for us when interpreting experimental data: a bell-shaped  $C - \phi_{\text{EDL}}$  curve from experiment may not be a certain indicator of highly dissociated electrolyte, instead, it may be a result of the formation and break-down of ion pairs (or larger ion clusters).

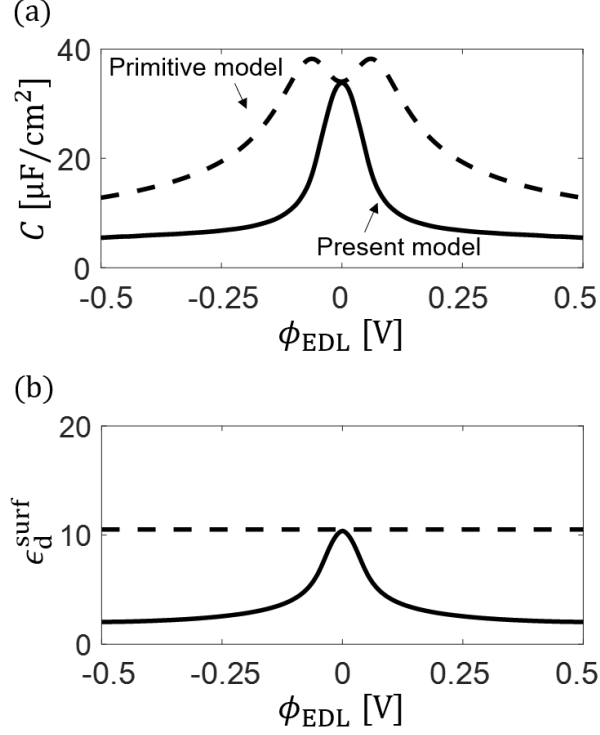


Figure 4. (a) Differential capacitance curves of the primitive model (dashed line) and present model (solid line).<sup>[14]</sup> In both cases,  $\gamma = 0.2$ . In the present model,  $p = 0.3 \cdot ea = 4.8 \cdot 10^{-29} \text{ C m}$ .  $T = 300 \text{ K}$ . (b) Field-dependent local dielectric constant at electrode | electrolyte interface vs electrode potential curve. Dashed line: primitive model; solid line: present model. In both cases,  $\gamma = 0.2$ . For both models,  $\epsilon_d$  is 10.5 in the bulk.

## Conclusions

In this work, we proposed a mean-field lattice-gas theory of the EDL in an IL system with transient paired ions bearing dipole moments. Using the analytical expression for the field-dependent local dielectric constant, we obtained the number density distribution of ion pairs, which was compared with MD simulations. Whereas the majority of ions in the bulk of solvent-free ionic liquids are bound, they shift to free state in the EDL, where the high electric field ‘prefers’ to interact with

free ions. The decrement of  $\epsilon_d$  at the electrode-electrolyte interface led to the reduction of the threshold of “camel-bell transition”; that is, even if the proportion of free charge carriers is lower than the ‘canonical threshold’,  $1/3$ , the  $C - \phi_{\text{EDL}}$  curve may well display a bell shape.

As mentioned in the Introduction, the model explored here is crude. Even using the concept of local dielectric constant at such distances is problematic (see multiple works on the nonlocal electrostatic theory of the electrical double layer).<sup>[51, 52]</sup> But as a qualitative signature of the effect, it sounds convincing: bound ions, for mere simplicity considered here as cation-anion pairs, are liberated into free states by the electric field inside the EDL.

## **Acknowledgement**

Y.Z. expresses his sincere gratitude to Dechun Si, Honghui Lv, Pedro de Souza and especially Xiaoyue Wang for discussions, suggestions, inspirations and encouragement. T.Y., M.C., and G.F. acknowledge the funding support from the National Natural Science Foundation of China (51876072). A.A.K. and Z.A.H.G. acknowledge discussion of various related issues with Michael Patrick McEldrew and Martin Bazant. J.H. acknowledges financial support from National Natural Science Foundation of China (21802170). Participation of Z.A.H.G in this work was supported through a studentship of the Centre for Doctoral Training on Theory and Simulation of Materials at Imperial College London, funded by the EPSRC (EP/L015579/1), and the funding from the Thomas Young Centre under grant number TYC-101. All MD simulations were performed at the National Supercomputing Centers in Guangzhou (Tianhe II). A.A.K. acknowledges funding from the Leverhulme Trust for (Grant No. RPG2016-223).



## Conflict of Interest

The authors declare no conflict of interest.

## Appendix

Taking the variation of the free energy density,  $f$ , with respect to  $n_i$  yields dimensionless electrochemical potential of cations and anions:

$$\mu_+ = \frac{e\phi}{k_B T} + \frac{1}{2} \ln \frac{\sinh\left(\frac{pE}{k_B T}\right)}{\frac{pE}{k_B T}} - \ln \frac{\left(\frac{n - n_+ - n_-}{2n_{\text{ref}}}\right)^{\frac{1}{2}}}{\frac{n_+}{n_{\text{ref}}}}, \quad (8)$$

$$\mu_- = -\frac{e\phi}{k_B T} + \frac{1}{2} \ln \frac{\sinh\left(\frac{pE}{k_B T}\right)}{\frac{pE}{k_B T}} - \ln \frac{\left(\frac{n - n_+ - n_-}{2n_{\text{ref}}}\right)^{\frac{1}{2}}}{\frac{n_-}{n_{\text{ref}}}}. \quad (9)$$

In the bulk, the electric field is totally screened and the electrostatic potential is taken to be zero; and we have  $n_+ = n_- = n_0 = \gamma n/2$  due to electric neutrality where  $n_0$  denotes the number density of cations (or anions) in the bulk.

Equalizing the electrochemical potential of each species to its counterpart in the bulk electrolyte, we obtain

$$\frac{e\phi}{k_B T} + \frac{1}{2} \ln \frac{\sinh\left(\frac{pE}{k_B T}\right)}{\frac{pE}{k_B T}} - \ln \frac{n_0}{n_+} \left(\frac{n - n_+ - n_-}{n - n_0 - n_0}\right)^{\frac{1}{2}} = 0, \quad (10)$$

$$-\frac{e\phi}{k_B T} + \frac{1}{2} \ln \frac{\sinh\left(\frac{pE}{k_B T}\right)}{\frac{pE}{k_B T}} - \ln \frac{n_0}{n_-} \left( \frac{n - n_+ - n_-}{n - n_0 - n_0} \right)^{\frac{1}{2}} = 0. \quad (11)$$

Note here  $n_{\text{ref}}$  is cancelled. Trivial rearrangements give

$$\exp\left(\frac{e\phi}{k_B T}\right) \left( \frac{\sinh\left(\frac{pE}{k_B T}\right)}{\frac{pE}{k_B T}} \right)^{\frac{1}{2}} = \frac{n_0}{n_+} \left( \frac{n - n_+ - n_-}{n - n_0 - n_0} \right)^{\frac{1}{2}}, \quad (12)$$

$$\exp\left(-\frac{e\phi}{k_B T}\right) \left( \frac{\sinh\left(\frac{pE}{k_B T}\right)}{\frac{pE}{k_B T}} \right)^{\frac{1}{2}} = \frac{n_0}{n_-} \left( \frac{n - n_+ - n_-}{n - n_0 - n_0} \right)^{\frac{1}{2}}. \quad (13)$$

To simplify further derivations, we will use a kind of interpolation approximation to the right-hand sides of these two equations. We brutally omit the square root there. Indeed the  $\left( \frac{n - n_+ - n_-}{n - n_0 - n_0} \right)^{\frac{1}{2}}$  and  $\frac{n - n_+ - n_-}{n - n_0 - n_0}$  have the same limiting behaviors: both are 0 when  $n_+ + n_- = n$ , and both are equal to 1 when  $n_+ + n_- = 2n_0$ . In between, this function would of course, be different, but the difference is not large and will not qualitatively affect the results. Such an approach has been used, in Ref. 19. We can then get simple analytical expressions for  $n_+$  and  $n_-$

$$\frac{n_+}{n} = \frac{n_0 \exp\left(-\frac{e\phi}{k_B T}\right)}{n_0 \exp\left(-\frac{e\phi}{k_B T}\right) + n_0 \exp\left(\frac{e\phi}{k_B T}\right) + (n - n_0 - n_0) \left( \frac{\sinh\left(\frac{pE}{k_B T}\right)}{\frac{pE}{k_B T}} \right)^{\frac{1}{2}}}, \quad (14)$$

$$\frac{n_-}{n} = \frac{n_0 \exp\left(\frac{e\phi}{k_B T}\right)}{n_0 \exp\left(-\frac{e\phi}{k_B T}\right) + n_0 \exp\left(\frac{e\phi}{k_B T}\right) + (n - n_0 - n_0) \left(\frac{\sinh\left(\frac{pE}{k_B T}\right)}{\frac{pE}{k_B T}}\right)^{\frac{1}{2}}}. \quad (15)$$

The number density expression for bound ions is given by  $n_{\text{bound}} = n - n_+ - n_-$  and is shown by Eq. (3).

*Derivation of the modified Poisson equation and field-dependent local dielectric constant*

Now, we develop the modified Poisson equation as well as the expression for  $\epsilon_d$ . Substituting the free energy functional into Euler-Lagrange equation  $\frac{\partial}{\partial x} \frac{\partial f}{\partial \phi'} - \frac{\partial f}{\partial \phi} = 0$ , we obtain

$$\epsilon_0 \epsilon_e \frac{dE}{dx} + \frac{d}{dx} \left( \frac{1}{2} (n - n_+ - n_-) p \mathcal{L}(pE/k_B T) \right) = e(n_+ - n_-), \quad (16)$$

where  $\mathcal{L}(s)$  is the Langevin function, defined in the main text. Rearrangement gives

$$\frac{d}{dx} \left( \epsilon_0 \left( \epsilon_e + \frac{(n - n_+ - n_-) p \mathcal{L}\left(\frac{pE}{k_B T}\right)}{2\epsilon_0 E} \right) E \right) = e(n_+ - n_-), \quad (17)$$

Finally, we obtain the modified Poisson equation

$$\frac{d}{dx} \left( \epsilon_0 \epsilon_d \frac{d\phi}{dx} \right) = -e(n_+ - n_-). \quad (18)$$

where  $\epsilon_d$  denotes the field-dependent local dielectric constant of the

system, given by

$$\epsilon_d = \epsilon_e + \frac{(n - n_+ - n_-)p\mathcal{L}\left(\frac{pE}{k_B T}\right)}{2\epsilon_0 E}. \quad (19)$$

## References

- [1] G. Wang, L. Zhang, J. Zhang, *Chem. Soc. Rev.* **2012**, 41, 797.
- [2] P. Simon, Y. Gogotsi, B. Dunn, *Science* **2014**, 343, 1210.
- [3] J. Luo, J. Liu, Z. Zeng, C. F. Ng, L. Ma, H. Zhang, J. Lin, Z. Shen, H. J. Fan, *Nano Lett.* **2013**, 13, 6136.
- [4] F. Endres, *Chem. Phys. Chem.* **2002**, 3, 144.
- [5] M. Galiński, A. Lewandowski, I. Stępnia, *Electrochim. Acta* **2006**, 51, 5567.
- [6] S. Zhang, J. Zhang, Y. Zhang, Y. Deng, *Chem. Rev.* **2017**, 117, 6755.
- [7] M. Fedorov, A. Kornyshev, *Chem. Rev.* **2014**, 114, 2978.
- [8] S. May, *Curr. Opin. Electrochem.* **2019**, 13, 125.
- [9] J. J. Bikerman, *London, Edinburgh Dublin Philos. Mag. J. Sci.* **1942**, 33, 384.
- [10] D. L. Chapman, *London, Edinburgh Dublin Philos. Mag. J. Sci.* **1913**, 25, 475.
- [11] V. Freise, *Z. Elektrochem.* **1952**, 56, 822.
- [12] M. Gouy, *J. Phys. Theor. Appl.* **1910**, 9, 457.
- [13] H. Helmholtz, *Ann. Phys.* **1879**, 243, 337.
- [14] A. Kornyshev, *J. Phys. Chem. B* **2007**, 111, 5545.

- [15] O. Stern, *Z. Elektrochem.* **1924**, 30, 508.
- [16] E. Wicke, M. Eigen, *Z. Elektrochem.* **1952**, 56, 551.
- [17] Z. Goodwin, G. Feng, A. Kornyshev, *Electrochim. Acta* **2017**, 225, 190.
- [18] Z. Goodwin, A. Kornyshev, *Electrochem. Commun.* **2017**, 82, 129.
- [19] J. Huang, *J. Phys. Chem. C* **2018**, 122, 3428.
- [20] Y. Zhang, J. Huang, *J. Phys. Chem. C* **2018**, 122, 28652.
- [21] A. Iglič, E. Gongadze, V. Kralj-Iglič, *Acta Chim. Slov.* **2019**, 66, 534.
- [22] P. Debye, *Polar molecules*, The Chemical Catalog Company, Inc.: New York, **1929**.
- [23] L. Onsager, *J. Am. Chem. Soc.* **1936**, 58, 1486.
- [24] J. Kirkwood, *J. Chem. Phys.* **1939**, 7, 911.
- [25] F. Booth, *J. Chem. Phys.* **1951**, 19, 391.
- [26] H. Fröhlich, A. Maradudin, *J. Phys. Today* **1959**, 12, 40.
- [27] J. Bockris, M. A. V. Devanathan, K. Müller, *Proc. Roy. Soc. A* **1963**, 274, 55.
- [28] J. Bockris, S. Khan, *Surface electrochemistry: a molecular level approach*, Springer Science & Business Media: **2013**.
- [29] W. Schmickler, E. Santos, *Interfacial Electrochemistry 2nd*,

Springer: **2010**.

- [30] R. M. Lynden-Bell, *Phys. Chem. Chem. Phys.* **2010**, *12*, 1733.
- [31] E. Gongadze, U. van Rienen, V. Kralj-Iglič, A. Iglič, *J. Comp. Method Biomec. Biomed. Eng.* **2013**, *16*, 463.
- [32] Y. Budkov, A. Kolesnikov, Z. Goodwin, M. Kiselev, A. Kornyshev, *Electrochim. Acta* **2018**, 284.
- [33] A. Levy, D. Andelman, H. Orland, *J. Chem. Phys.* **2013**, *139*, 164909.
- [34] R. Adar, T. Markovich, D. Andelman, *J. Chem. Phys.* **2017**, 146.
- [35] K. Ma, C. Lian, C. E. Woodward, B. Qin, *Chem. Phys. Lett.* **2020**, 739, 137001.
- [36] M. McEldrew, Z. Goodwin, A. Kornyshev, M. Z. Bazant, *J. Phys. Chem. Lett.* **2018**, *9*, 5840.
- [37] G. Feng, M. Chen, S. Bi, Z. Goodwin, E. Postnikov, N. Brilliantov, M. Urbakh, A. Kornyshev, *Phys. Rev. X* **2019**, *9*, 021024.
- [38] Y. Avni, R. M. Adar, D. Andelman, *Phys. Rev. E* **2020**, *101*, 010601.
- [39] B. B. Damaskin, A. N. Frumkin, *Electrochim. Acta* **1974**, *19*, 173.
- [40] R. Parsons, *J. Electroanal. Chem. Interfacial Electrochem.* **1975**, *59*, 229.
- [41] M. McEldrew, Z. Goodwin, S. Bi, M. Bazant, A. Kornyshev, *J. Chem. Phys.* **2020**, *152*, 234506.

- [42] J. Rigby, E. Izgorodina, *Phys. Chem. Chem. Phys.* **2013**, *15*, 1632.
- [43] M. Chen, Z. Goodwin, G. Feng, A. Kornyshev, *J. Electroanal. Chem.* **2017**, *819*, 347.
- [44] X. Jiang, R. Qiao, *J. Phys. Chem. C* **2012**, *116*, 1133.
- [45] S. Pronk, S. Páll, R. Schulz, P. Larsson, P. Bjelkmar, R. Apostolov, M. R. Shirts, J. C. Smith, P. M. Kasson, D. van der Spoel, B. Hess, E. Lindahl, *Bioinformatics* **2013**, *29*, 845.
- [46] T. Darden, D. York, L. Pedersen, *J. Chem. Phys.* **1993**, *98*, 10089.
- [47] G. Feng, J. Zhang, R. Qiao, *J. Phys. Chem. C* **2009**, *113*, 4549.
- [48] A. Lewandowski, A. Świdarska-Moczek, *J. Power Sources* **2009**, *194*, 601.
- [49] H. Xie, N. Gathergood, *Electrochemical Aspects of Ionic Liquids, 2nd Edition*, Wiley: **2012**.
- [50] Specifically, at -0.5 V, the first hump in simulation locates at 1 nm away from the electrode, because the first layer (0.5 nm) are filled with cations and the second layer (1.5 nm) anions (overscreening effect) with a certain portion of them forming ion pairs around 1nm. At -8 V, the first hump resides near 2 nm, almost 1 nm away from the first hump at -0.5 V. That is because the cations fill the second layer (overcrowding effect), therefore the ion pairs must be out of the second layer.
- [51] A. Kornyshev, M. Vorotyntsev, *Surf. Sci.* **1980**, *101*, 23.



- [52] A. Kornyshev, *Electrochim. Acta* **1981**, 26, 1.